

# We are IntechOpen, the world's leading publisher of Open Access books Built by scientists, for scientists

6,900

Open access books available

185,000

International authors and editors

200M

Downloads

Our authors are among the

154

Countries delivered to

TOP 1%

most cited scientists

12.2%

Contributors from top 500 universities



WEB OF SCIENCE™

Selection of our books indexed in the Book Citation Index  
in Web of Science™ Core Collection (BKCI)

Interested in publishing with us?  
Contact [book.department@intechopen.com](mailto:book.department@intechopen.com)

Numbers displayed above are based on latest data collected.  
For more information visit [www.intechopen.com](http://www.intechopen.com)



## Radiotracers for Molecular Imaging of Breast Cancer

Fan-Lin Kong and David J. Yang

*Department of Experimental Diagnostic Imaging,  
University of Texas MD Anderson Cancer Center, Houston, Texas  
USA*

### 1. Introduction

Breast cancer is the most prevailing malignancy among women in the world. 207,090 new cases of invasive breast cancer, along with 54,010 new cases of non-invasive types are expected to be diagnosed in women in the United States in 2010. Moreover, about 39,840 women are projected to die from this disease in the U.S in 2010. According to National Cancer Institute, the 5-year survival rate of breast cancer ranges from 23.4% in patients with stage IV to 98% in patients with stage I, highlighting the importance of early detection and diagnosis of this disease(American Cancer Society, 2010).

Molecular imaging does not only serve as an essential tool in breast cancer diagnosis and staging, but also provides significant amount of information for surgical management, radiation planning, chemotherapeutic assessment, and follow-up evaluation of patients. Currently, positron emission tomography (PET), single photon emission computed tomography (SPECT), and their combinations with CT, are major functional molecular imaging modalities used in clinic. Both PET and SPECT are based on the detection of radiolabeled ligands, termed "radiotracers", which are assumed to target tumor-specific characteristics at molecular levels. The accumulating understanding of the breast cancer molecular biology has highlighted pivotal factors that are critical for breast cancer progression, which allows researchers to select suitable targets for developing tumor-specific radiotracers. For instance, given that sustained tumor growth demands elevated glucose consumption for energy production in the lesion regions, PET radiotracer  $^{18}\text{F}$ -labeled glucose analog  $^{18}\text{F}$ -FDG has commonly been used to visualize the glucose metabolism of breast cancer cells(Buerkle & Weber, 2008). And yet,  $^{18}\text{F}$ -Fluoroestradiol is used to image estrogen receptor, which is highly overexpressed in a large proportion of breast tumor tissues(Jonson & Welch, 1998). Many other radiotracers have been designed to image cell proliferation, cell apoptosis, angiogenesis and hypoxia of breast tumors. Since breast cancer treatment has become more individualized in compliance with the distinct biological characteristics of tumors from each patient, the more target-specific molecular imaging radiotracers may play a key role to guide treatment selection and evaluate treatment response in the early stages.

This chapter has firstly been focused on two major molecular imaging modalities, PET and SPECT, their principles, limitations, as well as the typical radionuclides applied for those

modalities. The most commonly-used radiotracers,  $^{18}\text{F}$ -FDG for PET and  $^{99\text{m}}\text{Tc}$ -sestamibi for  $\gamma$ -imaging, have then been reviewed, respectively. In the following sections, we have discussed the radiotracers currently applied for breast cancer imaging other than  $^{18}\text{F}$ -FDG and  $^{99\text{m}}\text{Tc}$ -sestamibi, such as radiolabeled trastuzumab targeting HER2 receptor and  $^{18}\text{F}$ -fluorothymidine imaging cell proliferation. Those radiotracers have been described according to the categories of the tumor-specific targets.

## 2. Molecular imaging modalities and radionuclides

### 2.1 Positron emission tomography (PET) and its radionuclides

Positron emission tomography (PET) is a 3-D nuclear medicine imaging technique, which is based on detection of the annihilation radiation emitted from a certain positron-emitting radionuclide (Buerkle & Weber, 2008). When the radionuclide decays, the positron will annihilate with an electron nearby, thus create two 511 keV photons emitted opposite to each other (180 degree). This process is called “coincidence event”, which can be observed by PET detectors arranged in an array of full or partial ring around the patient body axis. Data are then reconstructed using standard algorithm. By using this coincidence-detection method, the traditional collimator of the SPECT scanner can be removed, therefore, the spatial resolution and sensitivity can be highly improved.

Commonly used PET imaging radionuclides are listed in Table 1. In order to monitor a small bioactive molecule *in vivo* without changing its chemical structure,  $^{11}\text{C}$  is often labeled as a substitute for the stable carbon atom  $^{12}\text{C}$  in that molecule. Given that  $^{11}\text{C}$  has only 20 min half-life,  $^{18}\text{F}$  can then be an alternative. In fact,  $^{18}\text{F}$  is currently the most frequently used/developed PET radionuclide. The best example of  $^{18}\text{F}$ -based radiotracers,  $^{18}\text{F}$ -labeled glucose analogue  $^{18}\text{F}$ -FDG, has been discussed in the next section. In addition to  $^{11}\text{C}$ - and  $^{18}\text{F}$ -labeled biomarkers, there are some other “non-targeted” radiotracers such as  $^{15}\text{O}$ -labeled water and  $^{13}\text{N}$ -labeled ammonia that measure blood flow in the patient body (Wijns & Camici, 1997). Moreover, copper-64 ( $^{64}\text{Cu}$ ) and zirconium-89 ( $^{89}\text{Zr}$ ), because of their long half-life (12.7 h and 78.4 h, respectively), have been increasingly recognized in the past decade for labeling nanoparticles or slowly localizing antibodies (DeNardo, 2005). Other than those cyclotron-produced PET radionuclides mentioned above, generator-produced gallium-68 ( $^{68}\text{Ga}$ ) and rubidium-82 ( $^{82}\text{Rb}$ ) have also shown high potentials in PET imaging. The advantage of in-house generator produced radionuclide is that generator itself serves as a top-of-the-bench source for short half-life radionuclides in the places that are located far from the cyclotron facility. Besides, it is quite simple to obtain radionuclides from the generator, and less expensive compared to cyclotron-produced radionuclides.

### 2.2 Single photon emission computed tomography (SPECT) and its radionuclides

Single photon emission computed tomography (SPECT) is a widely used nuclear medicine imaging modality, which utilizes radiotracers emitting gamma-ray photons directly from the labeling radionuclide. The energy of the radionuclide is generally from 70 to 364 keV (Table 2). A typical SPECT system consists of one or more rotating gamma camera(s) to obtain multiple projection images from different views around the patient, and a computer algorithm for 3D image reconstruction. A collimator is required to collect the  $\gamma$ -ray photons that only are emitted from the patient body in a particular direction (Benard & Turcotte, 2005).

Radionuclide	Half-life	Production
<sup>11</sup> C	20.4 min	Cyclotron
<sup>13</sup> N	9.97 min	Cyclotron
<sup>15</sup> O	2.03 min	Cyclotron
<sup>18</sup> F	109.7 min	Cyclotron
<sup>64</sup> Cu	12.8 h	Cyclotron
<sup>89</sup> Zr	78.4 h	Cyclotron
<sup>68</sup> Ga	68 min	Generator
<sup>82</sup> Rb	1.25 min	Generator

Table 1. Radionuclides commonly used in PET imaging.

Radionuclide	Decay Mode	Half-life	Emitted Photon Energy [keV]
<sup>99m</sup> Tc	IT	6.01 h	140 (87.7%)
<sup>201</sup> Tl	EC	73.0 h	71 (47%), 135 (3%), 167 (10%)
<sup>123</sup> I	EC	13.2 h	159 (83.3%)
<sup>131</sup> I	B <sup>-</sup>	8.02 d	364 (81.2%)
<sup>111</sup> In	EC	67.4 h	171(90.3%), 245 (94%)
<sup>67</sup> Ga	EC	78.3 h	93 (37%), 184 (20.4%), 300 (16.6%)

Table 2. Radionuclides commonly used in SPECT imaging (IT: isomeric transition, EC: electron capture).

Technetium-99m (<sup>99m</sup>Tc, t<sub>1/2</sub>=6.02 h) is the most common radionuclide for SPECT imaging. It emits a 140 keV gamma ray in 89% abundance, which can be detected by NaI detectors. In addition, it is produced with in-house generator that contains the parent nuclide molybdenum-99 (<sup>99</sup>Mo), and does not require the cyclotron. Since the chemistry of diagnostic radionuclide <sup>99m</sup>Tc is very similar to that of the therapeutic radioisotope rhenium-188 (<sup>188</sup>Re), they could be labeled to the same ligand, which leads to the diagnostic/therapeutic matched pair(Schechter et al., 2007).

Although the resolution and sensitivity of SPECT is not as good as PET scan due to its physical nature, SPECT and SPECT/CT still play important and irreplaceable roles in nuclear imaging area. First of all, SPECT radiopharmaceuticals are comparatively easier and less costly to produce. In addition, given that most SPECT radionuclides have longer half-life than PET radionuclides, SPECT offers more possibility to broaden the observational time window that allows the doctors to monitor biological processes *in vivo* several hours or even days after radiopharmaceutical administration. Furthermore, only limited facilities around the world can afford complete armamentarium of PET instruments and cyclotron for the local production of short-lived positron-emitters. Clinical data have shown that 15.9 million SPECT procedures were performed in 2007, while only 1.6 million of PET procedures were performed, in comparison (Mariani et al., 2008).

### 3. The most common radiotracers for breast cancer imaging in clinic

#### 3.1 $^{18}\text{F}$ -FDG for PET/CT and PEM (positron emission mammography)

In recent years,  $^{18}\text{F}$ -fluoro-deoxy-glucose ( $^{18}\text{F}$ -FDG), which is an  $^{18}\text{F}$ -labeled analog of glucose, has become the most common and attractive radiotracer for PET scans. Both  $^{18}\text{F}$ -FDG and glucose are transported across the cell membrane by glucose transporters.  $^{18}\text{F}$ -FDG is phosphorylated by hexokinase to  $^{18}\text{F}$ -FDG-6-phosphate while glucose is phosphorylated to glucose-6-phosphate. Unlike glucose-6-phosphate,  $^{18}\text{F}$ -FDG-6-phosphate cannot be further metabolized, and therefore, is trapped and accumulates steadily in the tumor cells (Buerkle & Weber, 2008). Hence,  $^{18}\text{F}$ -FDG is able to provide high sensitivity and specificity for detecting, staging, and restaging tumors by imaging high glucose metabolic rates in tumor cells. For breast cancer cells, increased glucose utilization is caused by the overexpression of glucose transporters Glut-1/3 and increased hexokinase activity. The rate-limiting step in the uptake of  $^{18}\text{F}$ -FDG in breast cancer appears to be the phosphorylation process by hexokinase, particularly hexokinase I (Buck et al., 2004).

Although  $^{18}\text{F}$ -FDG-PET generally has high sensitivity and specificity in detecting malignancies, whole-body  $^{18}\text{F}$ -FDG-PET is not quite suitable for primary breast cancer diagnosis, especially for the low grade tumors and tumors with a size less than 1 cm in diameter (Lim et al., 2007). In addition, it is not appropriate for breast cancer screening as well. Therefore,  $^{18}\text{F}$ -FDG with positron emission mammography (PEM) has been introduced as an alternative. In comparison with PET, PEM has a much higher spatial resolution by putting two opposite detector heads on each side of the breast and thus minimizing the distance between radiation source and the detectors. Schilling *et al.* have reported that PEM can detect tumor as small as 1.5 mm in diameter, with much less breast compression compared to traditional mammography (Schilling et al., 2011). They have also indicated that PEM is not affected by breast density and it has good sensitivity (90%) in detecting ductal carcinoma *in situ* (DCIS), which cannot be detected by PET very well.

For breast cancer logoregional staging,  $^{18}\text{F}$ -FDG-PET has shown high sensitivity in axillary staging of late-stage cancer patients, but not sensitive enough in detecting the early-stage micrometastases and small tumor-infiltrated axillary lymph nodes (Aukema et al., 2010). Therefore,  $^{18}\text{F}$ -FDG-PET is not sufficient to replace the sentinel lymph node (SLN) biopsy in this case. Instead,  $^{18}\text{F}$ -FDG-PET appears to be suitable for distant (systemic) staging, as well as for staging locally advanced breast cancer (LABC) because LABC usually has large primary tumor (> 5 cm in diameter) or advanced axillary disease without clinically apparent distant metastases (Mahner et al., 2008). Moreover, several studies have demonstrated that

$^{18}\text{F}$ -FDG-PET is superior to traditional bone scintigraphy in the detection of osteolytic and intramedullary metastases but inferior in the detection of primary osteoblastic lesions (Schirrmeyer, 2007).

An increasing number of studies have been performed to evaluate treatment response using  $^{18}\text{F}$ -FDG-PET. Although  $^{18}\text{F}$ -FDG has not been recommended as a routine assessment agent yet, it has been proven to be an accurate early predictor of poor response to therapy. Patients with a high  $^{18}\text{F}$ -FDG uptake associated with low blood flow/perfusion rate in their tumors were more likely to have poor response and early relapse (Tseng et al., 2004).

### 3.2 $^{99\text{m}}\text{Tc}$ -sestamibi for scintimammography and BSGI (breast-specific $\gamma$ -imaging)

$^{99\text{m}}\text{Tc}$ -methoxyisobutylisonitrile ( $^{99\text{m}}\text{Tc}$ -MIBI or  $^{99\text{m}}\text{Tc}$ -sestamibi) scintimammography has been increasingly used to assess the suspicious lesions of patients with a negative or indeterminate mammography in the clinic (Filippi et al., 2006). This small lipophilic cation was originally developed as a myocardial perfusion agent. The first report of its application in breast cancer detection was by Aktolun *et al.* in 1992 (Aktolun et al., 1992). The cellular uptake mechanisms of  $^{99\text{m}}\text{Tc}$ -sestamibi still remain unclear; however, its uptake is driven by a negative transmembrane potential and most of the radioactivity is found in the mitochondria (Scopinaro et al., 1994).  $^{99\text{m}}\text{Tc}$ -sestamibi scintimammography shows higher sensitivity (85%) and specificity (87%) than the traditional mammography, and its sensitivity is independent of breast density (Lieberman et al., 2003). In addition,  $^{99\text{m}}\text{Tc}$ -sestamibi is a substrate of the transmembrane P-glycoprotein (Pgp), which is a member of the MDR/TAP subfamily that is involved in the multidrug resistance. Therefore, the uptake, clearance, and retention of  $^{99\text{m}}\text{Tc}$ -sestamibi have been investigated as predictors of response to chemotherapy in human breast cancer (Kim et al., 2006). In a study of 45 patients with primary breast cancer, Cayre *et al.* concluded that a negative  $^{99\text{m}}\text{Tc}$ -sestamibi scintimammography predicted chemoresistance with a specificity of 100%. Besides,  $^{99\text{m}}\text{Tc}$ -sestamibi uptake was inversely correlated to the expression of multidrug resistance protein MDR1 ( $P < 0.05$ ) in invasive ductal carcinomas (Cayre et al., 2002).

Nevertheless,  $^{99\text{m}}\text{Tc}$ -sestamibi scintimammography demonstrates relatively low sensitivity in detecting the nonpalpable lesions or tumors smaller than 1 cm. Therefore, the high resolution small field-of-view breast-specific  $\gamma$ -imaging (BSGI) has been developed as an alternative. Similar to PEM, the single-head detector used in BSGI is mounted opposite to a compression plate, so the patient's breast is compressed between detector and plate. According to a 6-year BSGI study performed by Hruska *et al.* at Mayo Clinic, the sensitivity of BSGI for tumors larger than 1 cm was 97%, while that for tumors smaller than 1 cm was 74% (Hruska et al., 2008). When compare BSGI with PEM, although the average sensitivity of PEM (93%) is slightly higher than that of BSGI (89%), BSGI has a much higher negative predictive value (100%) than that of PEM (88%) (Ferrara, 2010). Thus, both of the imaging modalities have great detection ability in existing studies, and there is no proven clinically significant advantage to either modality over the other so far.

## 4. Other radiotracers imaging breast cancer molecular biomarkers

### 4.1 Radiotracer targeting hormone receptors

#### $^{18}\text{F}$ -Fluoroestradiol ( $^{18}\text{F}$ -FES) targets Estrogen receptor (ER)

More than 70% of the breast tumors are positive for hormone receptors such as estrogen receptor (ER+), and ER-directed breast cancer therapeutic agents such as tamoxifen and

aromatase inhibitors are highly effective to these patients with fewer side effects, while compared to the traditional chemotherapy (Oude Munnink et al., 2009). To date,  $^{18}\text{F}$ -16 $\alpha$ -17 $\beta$ -fluoroestradiol ( $^{18}\text{F}$ -FES) has been proven to be the most successful PET radiotracer in determining ER status and prognosis of ER-directed hormonal therapy in breast cancer patients (Jonson & Welch, 1998).

For clinical use, an automated synthesis of  $^{18}\text{F}$ -FES can be achieved in a decay-corrected yield of 30% at 60 minutes after end of bombardment with high radiochemical purity (>99%) (Romer et al., 2001).  $^{18}\text{F}$ -FES has a high binding affinity to ER, especially the ER $\alpha$  subtype (Yoo et al., 2005). In both human and rodents,  $^{18}\text{F}$ -FES is rapidly taken up and metabolized by the liver. By 20 min after injection, 80% of the  $^{18}\text{F}$ -FES is converted to radiolabeled glucuronide and sulfate conjugates in blood. The recommended injection dose and imaging time of  $^{18}\text{F}$ -FES is 6mCi at 30 min after injection (Sundararajan et al., 2007). Peterson *et al* demonstrated excellent agreement ( $r=0.99$ ) between  $^{18}\text{F}$ -FES-PET and ER expression assayed by immunohistochemistry (IHC) in 17 patients. In addition, their study indicated that ER- tumors in those patients had partial-volume-corrected SUV of less than 1.0, while that of ER+ tumors were above 1.1 (Peterson et al., 2008).

## 4.2 Radiotracers imaging HER 2

### Radiolabeled trastuzumab

Human epidermal growth factor receptor 2 (HER2) is a transmembrane glycoprotein that forms heterodimers with other EGFR family members to activate distinct signaling pathways, which are involved in cell growth, survival, differentiation, adhesion, and migration. HER2 has been found to be overexpressed in many types of cancers. For breast cancer patients, about 25-30% of breast tumors have HER2/*neu* gene amplification and/or HER2 protein overexpression (Moasser, 2007). Therefore, HER2 has become an attractive target for breast cancer imaging and treatment. The humanized monoclonal antibody trastuzumab has been successfully used for HER2-positive breast cancer treatment. By labeling trastuzumab with different radionuclides, we can assess the HER2 expression and localization in breast cancer patients non-invasively, and thus, select the patients with HER2-positive tumors that are qualified for trastuzumab treatment (Capala & Bouchelouche, 2010).

Zirconium-89 ( $^{89}\text{Zr}$ ;  $t_{1/2}=78.41$  h) has been chosen for trastuzumab labeling because it has the longest half-life among the positron-emitting radionuclides, which allows PET imaging up to 7 days after injection (Holland et al., 2009). The antibodies like trastuzumab often have high molecular weight, thus slow metabolism and clearance. Hence, longer half-life radionuclides are more suitable to obtain better tumor-to-blood ratios even several days post injection. Dijkers *et al* have performed their first clinical trial of  $^{89}\text{Zr}$ -trastuzumab PET in 14 patients with HER2-positive metastatic breast cancer. They have determined the optimal imaging time and dose as 4-5 days post injection and 50 mg dose for trastuzumab-naïve patients or 10 mg dose for patients already on trastuzumab treatment, respectively (Dijkers et al., 2010). Other than  $^{89}\text{Zr}$ , trastuzumab has also been labeled with  $^{124}\text{I}$ ,  $^{86}\text{Y}$ , and  $^{76}\text{Br}$  for PET (Orlova et al., 2009; Winberg et al., 2004; Xu et al., 2007). In addition, the antibody has been labeled with  $^{111}\text{In}$  for SPECT imaging (Sampath et al., 2007). To date, only  $^{89}\text{Zr}$  and  $^{111}\text{In}$ -labeled trastuzumab have been applied to human in the clinical trials. Although the tumor uptake levels of  $^{89}\text{Zr}$ -trastuzumab and  $^{111}\text{In}$ -trastuzumab were similar,  $^{89}\text{Zr}$ -labeled counterpart demonstrated better image quality due to higher spatial resolution and sensitivity of PET.

### 4.3 Radiotracer imaging cell proliferation

#### <sup>18</sup>F-fluorothymidine (18F-FLT)

<sup>18</sup>F-fluoro-3'-deoxy-3'-L-fluorothymidine (<sup>18</sup>F-FLT) is a nucleoside-based radiotracer that was developed to target DNA replication and cell proliferation in tumors in 1998(Shields et al., 1998). <sup>18</sup>F-FLT enters the tumor cells mainly by Na<sup>+</sup>-dependent active nucleoside transporters, which are generally upregulated in tumor cells(Reske & Deisenhofer, 2006). The same as thymidine, <sup>18</sup>F-FLT follows the salvage pathway of DNA synthesis and undergoes phosphorylation by thymidine kinase 1 (TK1). Since the 3'-hydroxyl group is converted to 3'-fluorine, <sup>18</sup>F-FLT cannot be incorporated into DNA and is trapped in cytosol(Seitz et al., 2002). Therefore, the rate-limiting step for <sup>18</sup>F-FLT-PET imaging is phosphorylation by TK1. TK1 has little activity in the quiescent cells but increased activity in proliferating cells, especially in the cells in S-phase(Munch-Petersen et al., 1995).

In clinical studies, <sup>18</sup>F-FLT-PET is commonly used in detecting brain tumor given its low uptake in the normal brain tissue(Spence et al., 2009). The high uptake in bone marrow and liver limits its diagnostic application especially in the assessment of liver and bone metastases. Besides, <sup>18</sup>F-FLT-PET is not superior to <sup>18</sup>F-FDG for cancer staging due to its low tumor-to-background ratios. Therefore, the imaging potential of <sup>18</sup>F-FLT in breast cancer has been evaluated more often in the prediction and assessment of tumor response to a certain treatment. For instance, Pio *et al* scanned 14 breast cancer patients before and two weeks after the first cycle of the treatment, and found out that <sup>18</sup>F-FLT uptake was strongly correlated with percentage change in CA27.29 tumor marker levels ( $r = 0.79$ ;  $p = 0.001$ ). In addition, the <sup>18</sup>F-FLT uptake change after the chemotherapy course was predictive of late change in tumor size ( $r = 0.74$ ;  $p = 0.01$ ) as measured by CT scans(Pio et al., 2006). In a more recent study, Kenny *et al* assessed <sup>18</sup>F-FLT response to a combined chemotherapy using 5-fluorouracil, epirubicin, and cyclophosphamide in 13 breast cancer patients with 17 discrete lesions. Their observations indicated a significant difference in <sup>18</sup>F-FLT uptake change between the responders and non-responders. The average decrease in responding lesions at 90 min were 41.3% for SUV and 52.9% for Ki (net irreversible plasma to tumor transfer constant), while those of non-responding lesions were 3.1% and 1.9%, respectively(Kenny et al., 2007).

To meet the clinical application needs, however, significant improvements are required in <sup>18</sup>F-FLT radiosynthesis. So far, there are two synthesis methods using different precursors, but neither could achieve an optimal radiochemical yield within a short preparation time. By using precursor 3'-O-nosyl thymidine with its pyrimidine ring protected with N-BOC, Yun *et al* achieved a high radiochemical yield of  $42 \pm 5.4\%$  within 60 min in a radiochemical purity  $>97\%$ (Yun et al., 2003). On the other hand, Machulla *et al* used 5'-O-(4,4'-dimethoxytriphenylmethyl)-2,3'-anhydrothymidine (DMTThy) as the precursor to achieve the preparation time within 10 min at 160°C, however, the radiochemical yield was only  $14.3 \pm 3.3\%$ (Machulla et al., 2000).

### 4.4 Radiotracers imaging amino acid transporters and protein synthesis

#### <sup>11</sup>C/<sup>99m</sup>Tc-methionine

Amino acid-based radiotracers are developed for tumor imaging based on the fact that tumor cells uptake and consume more amino acids to sustain their uncontrolled growth compared with the normal cells. Most of those radiotracers are reported to enter the tumor

cells via amino acid transporters, such as Na<sup>+</sup>-independent L-type amino acid transporter system LAT, and Na<sup>+</sup>-dependent transport systems A and B<sup>0</sup>(Jager et al., 2001).

<sup>11</sup>C-methionine (<sup>11</sup>C-MET) can be synthesized with an automation module within 20 min after the bombardment in a radiochemical yield of >30%. The specific activity was 3.3 Ci/mmol, and the radiochemical purity was >96%(Davis et al., 1982). <sup>11</sup>C-MET has recently been evaluated by Lindholm *et al* for its potential in assessing early response to therapy in advanced breast cancer. Twenty-five out of 26 metastatic sites from 13 patients could be detected by <sup>11</sup>C-MET-PET. The standard uptake value (SUV) in all six responding metastatic sites decreased by 30-54% (P <0.05), while that of non-responding sites did not decrease significantly (11-13%; P =NS)(Lindholm et al., 2009).

On the other hand, <sup>99m</sup>Tc-labeled methionine has also been successfully used to detect breast cancer in a recent clinical trial performed by Sharma *et al*. <sup>99m</sup>Tc-methionine is proven to have the same biological properties as <sup>11</sup>C-methionine, but the longer half-life of in-house generator-produced radioisotope <sup>99m</sup>Tc (t<sub>1/2</sub> =6 h) provides a more simple and affordable way to image breast tumor using conventional scintimammography. <sup>99m</sup>Tc-methionine was synthesized by conjugating methionine with diethylene triamine pentaacetic acid and <sup>99m</sup>Tc, and the radiochemical yield was >95%. The sensitivity, specificity, and positive predictive value of <sup>99m</sup>Tc-methionine in this clinical trial with 47 patients were 87.8%, 92.8%, and 96.6%, respectively(Sharma et al., 2009).

#### 4.5 Radiotracers imaging angiogenesis

##### Radiolabeled RGD peptides

Angiogenesis, which stands for the formation of new blood vessels, is required for solid tumor to obtain essential oxygen and nutrients for growth. Integrins, one kind of glycoproteins located on the cell surface, are extremely important in angiogenesis to mediate cell-cell or cell-extracellular matrix interactions(Takada et al., 2007). There are 24 integrins being reported up to date; among these, integrin  $\alpha_v\beta_3$  is the best-studied subtype as the molecular marker for targeting angiogenic cascade. A small peptide sequence consists of arginine-glycine-aspartic acid (RGD) has been identified as the motif of integrins for binding to their  $\alpha_v$  subunit, including  $\alpha_v\beta_3$ (Ruoslahti & Pierschbacher, 1987). Several radiolabeled RGD peptides have been developed to image breast tumors in human. Here, two major radiotracers are introduced, <sup>99m</sup>Tc-NC100692 for SPECT imaging and <sup>18</sup>F-galacto-RGD for PET imaging.

NC100692 is a cyclic synthetic ligand containing RGD binding site with high affinity to  $\alpha_v\beta_3$  and  $\alpha_v\beta_5$ , which are upregulated during angiogenesis. <sup>99m</sup>Tc-NC100692 is currently under Phase II clinical trial by GE healthcare. In the study performed by Bach-Gansmo *et al*, 19 out of 22 malignant lesions from 20 breast cancer patients were detected by <sup>99m</sup>Tc-NC100692 scintigraphy (86%)(Bach-Gansmo et al., 2006). In the Phase 2a study performed by Axelsson *et al*, <sup>99m</sup>Tc-NC100692 scintigraphy detected 1 out of 7 liver, 4 out of 5 lung, 8 out of 17 bone, and 1 out of 1 brain metastases in 10 patients with breast cancer(Axelsson et al., 2010).

<sup>18</sup>F-galacto-RGD was first developed by Haubner *et al* in 2001(Haubner et al., 2001). By adding a sugar amino acid to the RGD peptide, the lipophilicity of the tracer could be reduced, which resulted in less uptake in liver and increased uptake in tumor. The overall radiochemical yield of <sup>18</sup>F-galacto-RGD was 29±5%, and the purity was >98%(Haubner et al., 2004). Beer *et al* performed <sup>18</sup>F-galacto-RGD-PET in 16 patients with invasive ductal breast cancer in 2007. All of the invasive carcinomas could be identified (SUV = 3.6±1.8, tumor-to-muscle ratios = 6.2±2.2), however, only 3 out of 8 lymph node metastases were detected(Beer

et al., 2008). In addition,  $^{18}\text{F}$ -galacto-RGD images were found to represent the mixture of  $\alpha_v\beta_3$  expressed in both tumor cells and endothelial cells, so the agent was not tumor specific. According to several preclinical and clinical studies,  $^{18}\text{F}$ -galacto-RGD-PET may not be suitable to differentiate tumor from inflammation, because  $\alpha_v\beta_3$  is also highly expressed in the macrophages and other inflammatory lesions (Gaertner et al., 2010).

#### 4.6 Radiotracers for bone scan

##### $^{99\text{m}}\text{Tc}$ -methylene diphosphonate ( $^{99\text{m}}\text{Tc}$ -MDP)

The most common site of breast cancer metastases is bone, mainly spine and pelvis. The distribution of bone metastases is a prognostic factor of breast cancer (Hamaoka et al., 2004). Bone scintigraphy using  $^{99\text{m}}\text{Tc}$ -methylene diphosphonate ( $^{99\text{m}}\text{Tc}$ -MDP) is the standard initial imaging technique to assess bone metastases. The uptake mechanism of  $^{99\text{m}}\text{Tc}$ -MDP in bone is the chemical absorption onto the surface of hydroxyapatite and then incorporation into the crystalline structure of hydroxyapatite (Kanishi, 1993). The specificity and sensitivity of  $^{99\text{m}}\text{Tc}$ -MDP bone scintigraphy for breast cancer bone metastases are 78-100% and 62-100%, respectively (Hamaoka et al., 2004). Since its detection rate in early stages breast cancer patient is very low (0.82% for stage I disease), the routine screening is only recommended to patients in advanced stages (Yeh et al., 1995). In addition,  $^{99\text{m}}\text{Tc}$ -MDP bone scintigraphy may not be suitable to monitor hormonal therapy response because of the increased  $^{99\text{m}}\text{Tc}$ -MDP uptake caused by new bone formation during the repair process after the therapy ("flare phenomenon") (Mortimer et al., 2001). In summary, given its high availability and affordability, as well as its rapid generation of whole-body images, the advantage of bone scintigraphy is rather for screening the patient with late stage (III and IV) breast cancer, than diagnosis. Instead of bone scintigraphy,  $^{99\text{m}}\text{Tc}$ -MDP using SPECT or SPECT/CT is more suitable for the diagnosis of breast cancer bone metastases given its higher resolution and accuracy. The specificity and sensitivity of  $^{99\text{m}}\text{Tc}$ -MDP-SPECT are 91-93% and 87-92%, respectively (Han et al., 1998).

##### $^{18}\text{F}$ -fluoride

$^{18}\text{F}$ -labeled sodium fluoride ( $^{18}\text{F}$ -fluoride) is a non-specific PET radiotracer for whole-body bone metastases imaging. Its uptake is via the exchange of hydroxyl ions in the hydroxyapatite crystal, mainly at the surface of the skeleton (Hawkins et al., 1992).  $^{18}\text{F}$ -fluoride PET has higher resolution, sensitivity (99%) and specificity (97%) than  $^{99\text{m}}\text{Tc}$ -MDP-SPECT (Even-Sapir et al., 2004). Besides, the absolute uptake of  $^{18}\text{F}$ -fluoride in normal bone was twice as high as that of  $^{99\text{m}}\text{Tc}$ -MDP. Although  $^{18}\text{F}$ -fluoride is not tumor-specific, it can differentiate tumor from benign tissues better than  $^{99\text{m}}\text{Tc}$ -MDP bone scintigraphy thanks to the superior spatial resolution of PET scanner. Among all the benign abnormalities detected by  $^{18}\text{F}$ -fluoride PET, 80% are caused by endplate fractures and arthritis of the articular facets, both of which have a typical uptake pattern of  $^{18}\text{F}$ -fluoride (Schirrmeyer et al., 1998). In  $^{18}\text{F}$ -fluoride PET images, lesions that are not located at joint surfaces are suspicious for metastases. In addition, the lesions that do not show the typical pattern of endplate fracture, osteophytes, or serial rib fractures are suspicious for metastases as well.

#### 5. Conclusion

Molecular imaging such as PET and SPECT plays an important role in non-invasive breast cancer diagnosis, staging, and treatment response evaluation. In this chapter, we have

focused on introducing the radiotracers commonly used in molecular imaging of breast cancer, according to the classification of the tumor-specific characteristics to which they are targeting. To date,  $^{18}\text{F}$ -FDG and  $^{99\text{m}}\text{Tc}$ -sestamibi are still the two most extensively used radiopharmaceuticals in breast cancer for PET and  $\gamma$ -imaging, respectively. The advances in molecular cancer biology have led to an increased understanding of the cancer biomarkers that contribute to cancer progression, and thus led to the rapid development of more personalized and specifically tumor-targeted treatments. There is an increasing demand on molecular imaging and tracer development to help direct and assess the treatment response in an early stage.

## 6. References

- Aktolun, C., Bayhan, H. & Kir, M. (1992). "Clinical experience with Tc-99m MIBI imaging in patients with malignant tumors. Preliminary results and comparison with Tl-201." *Clin Nucl Med* 17(3): 171-176
- American Cancer Society. (2010, n.d.). "Breast Cancer Facts & Figures 2009-2010." from <http://www.cancer.org/acs/groups/content/@nho/documents/document/f861009final90809pdf.pdf>.
- Aukema, T. S., Rutgers, E. J., Vogel, W. V., Teertstra, H. J., Oldenburg, H. S., Vrancken Peeters, M. T., Wesseling, J., Russell, N. S. & Valdes Olmos, R. A. (2010). "The role of FDG PET/CT in patients with locoregional breast cancer recurrence: a comparison to conventional imaging techniques." *Eur J Surg Oncol* 36(4): 387-392
- Axelsson, R., Bach-Gansmo, T., Castell-Conesa, J. & McParland, B. J. (2010). "An open-label, multicenter, phase 2a study to assess the feasibility of imaging metastases in late-stage cancer patients with the alpha v beta 3-selective angiogenesis imaging agent  $^{99\text{m}}\text{Tc}$ -NC100692." *Acta Radiol* 51(1): 40-46
- Bach-Gansmo, T., Danielsson, R., Saracco, A., Wilczek, B., Bogsrud, T. V., Fangberget, A., Tangerud, A. & Tobin, D. (2006). "Integrin receptor imaging of breast cancer: a proof-of-concept study to evaluate  $^{99\text{m}}\text{Tc}$ -NC100692." *J Nucl Med* 47(9): 1434-1439
- Beer, A. J., Niemeyer, M., Carlsen, J., Sarbia, M., Nahrig, J., Watzlowik, P., Wester, H. J., Harbeck, N. & Schwaiger, M. (2008). "Patterns of alphavbeta3 expression in primary and metastatic human breast cancer as shown by  $^{18}\text{F}$ -Galacto-RGD PET." *J Nucl Med* 49(2): 255-259
- Benard, F. & Turcotte, E. (2005). "Imaging in breast cancer: Single-photon computed tomography and positron-emission tomography." *Breast Cancer Res* 7(4): 153-162
- Buck, A. K., Schirrmeister, H., Mattfeldt, T. & Reske, S. N. (2004). "Biological characterisation of breast cancer by means of PET." *Eur J Nucl Med Mol Imaging* 31 Suppl 1: S80-87
- Buerkle, A. & Weber, W. A. (2008). "Imaging of tumor glucose utilization with positron emission tomography." *Cancer Metastasis Rev* 27(4): 545-554
- Capala, J. & Bouchelouche, K. (2010). "Molecular imaging of HER2-positive breast cancer: a step toward an individualized 'image and treat' strategy." *Curr Opin Oncol* 22(6): 559-566
- Cayre, A., Cachin, F., Maublant, J., Mestas, D., Feillel, V., Ferriere, J. P., Kwiaktowski, F., Chevillard, S., Finat-Duclos, F., Verrelle, P. & Penault-Llorca, F. (2002). "Single static view  $^{99\text{m}}\text{Tc}$ -sestamibi scintimammography predicts response to neoadjuvant chemotherapy and is related to MDR expression." *Int J Oncol* 20(5): 1049-1055

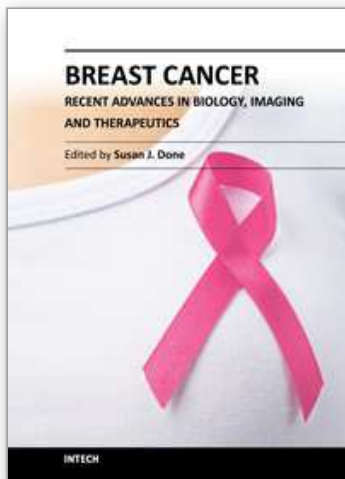
- Davis, J., Yano, Y., Cahoon, J. & Budinger, T. F. (1982). "Preparation of  $^{11}\text{C}$ -methyl iodide and L-[S-methyl- $^{11}\text{C}$ ]methionine by an automated continuous flow process." *Int J Appl Radiat Isot* 33(5): 363-369
- DeNardo, S. J. (2005). "Radioimmunodetection and therapy of breast cancer." *Semin Nucl Med* 35(2): 143-151
- Dijkers, E. C., Oude Munnink, T. H., Kosterink, J. G., Brouwers, A. H., Jager, P. L., de Jong, J. R., van Dongen, G. A., Schroder, C. P., Lub-de Hooge, M. N. & de Vries, E. G. (2010). "Biodistribution of  $^{89}\text{Zr}$ -trastuzumab and PET imaging of HER2-positive lesions in patients with metastatic breast cancer." *Clin Pharmacol Ther* 87(5): 586-592
- Even-Sapir, E., Metser, U., Flusser, G., Zuriel, L., Kollender, Y., Lerman, H., Lievshitz, G., Ron, I. & Mishani, E. (2004). "Assessment of malignant skeletal disease: initial experience with  $^{18}\text{F}$ -fluoride PET/CT and comparison between  $^{18}\text{F}$ -fluoride PET and  $^{18}\text{F}$ -fluoride PET/CT." *J Nucl Med* 45(2): 272-278
- Ferrara, A. (2010). "Nuclear imaging in breast cancer." *Radiol Technol* 81(3): 233-246
- Filippi, L., Pulcini, A., Remediani, S., Masci, E., Redler, A., Scopinaro, F. & De Vincentis, G. (2006). "Usefulness of scintimammography with  $^{99\text{m}}\text{Tc}$  MIBI in clinical practice." *Clin Nucl Med* 31(12): 761-763
- Gaertner, F. C., Schwaiger, M. & Beer, A. J. (2010). "Molecular imaging of avb3 expression in cancer patients." *Q J Nucl Med Mol Imaging*
- Hamaoka, T., Madewell, J. E., Podoloff, D. A., Hortobagyi, G. N. & Ueno, N. T. (2004). "Bone imaging in metastatic breast cancer." *J Clin Oncol* 22(14): 2942-2953
- Han, L. J., Au-Yong, T. K., Tong, W. C., Chu, K. S., Szeto, L. T. & Wong, C. P. (1998). "Comparison of bone single-photon emission tomography and planar imaging in the detection of vertebral metastases in patients with back pain." *Eur J Nucl Med* 25(6): 635-638
- Haubner, R., Kuhnast, B., Mang, C., Weber, W. A., Kessler, H., Wester, H. J. & Schwaiger, M. (2004). "[ $^{18}\text{F}$ ]Galacto-RGD: synthesis, radiolabeling, metabolic stability, and radiation dose estimates." *Bioconjug Chem* 15(1): 61-69
- Haubner, R., Wester, H. J., Weber, W. A., Mang, C., Ziegler, S. I., Goodman, S. L., Senekowitsch-Schmidtke, R., Kessler, H. & Schwaiger, M. (2001). "Noninvasive imaging of  $\alpha(v)\beta_3$  integrin expression using  $^{18}\text{F}$ -labeled RGD-containing glycopeptide and positron emission tomography." *Cancer Res* 61(5): 1781-1785
- Hawkins, R. A., Choi, Y., Huang, S. C., Hoh, C. K., Dahlbom, M., Schiepers, C., Satyamurthy, N., Barrio, J. R. & Phelps, M. E. (1992). "Evaluation of the skeletal kinetics of fluorine-18-fluoride ion with PET." *J Nucl Med* 33(5): 633-642
- Holland, J. P., Sheh, Y. & Lewis, J. S. (2009). "Standardized methods for the production of high specific-activity zirconium-89." *Nucl Med Biol* 36(7): 729-739
- Hruska, C. B., Boughey, J. C., Phillips, S. W., Rhodes, D. J., Wahner-Roedler, D. L., Whaley, D. H., Degnim, A. C. & O'Connor, M. K. (2008). "Scientific Impact Recognition Award: Molecular breast imaging: a review of the Mayo Clinic experience." *Am J Surg* 196(4): 470-476
- Jager, P. L., Vaalburg, W., Pruim, J., de Vries, E. G., Langen, K. J. & Piers, D. A. (2001). "Radiolabeled amino acids: basic aspects and clinical applications in oncology." *J Nucl Med* 42(3): 432-445
- Jonson, S. D. & Welch, M. J. (1998). "PET imaging of breast cancer with fluorine-18 radiolabeled estrogens and progestins." *Q J Nucl Med* 42(1): 8-17

- Kanishi, D. (1993). "<sup>99m</sup>Tc-MDP accumulation mechanisms in bone." *Oral Surg Oral Med Oral Pathol* 75(2): 239-246
- Kenny, L., Coombes, R. C., Vigushin, D. M., Al-Nahhas, A., Shousha, S. & Aboagye, E. O. (2007). "Imaging early changes in proliferation at 1 week post chemotherapy: a pilot study in breast cancer patients with 3'-deoxy-3'-[<sup>18</sup>F]fluorothymidine positron emission tomography." *Eur J Nucl Med Mol Imaging* 34(9): 1339-1347
- Kim, I. J., Bae, Y. T., Kim, S. J., Kim, Y. K., Kim, D. S. & Lee, J. S. (2006). "Determination and prediction of P-glycoprotein and multidrug-resistance-related protein expression in breast cancer with double-phase technetium-99m sestamibi scintimammography. Visual and quantitative analyses." *Oncology* 70(6): 403-410
- Liberman, M., Sampalis, F., Mulder, D. S. & Sampalis, J. S. (2003). "Breast cancer diagnosis by scintimammography: a meta-analysis and review of the literature." *Breast Cancer Res Treat* 80(1): 115-126
- Lim, H. S., Yoon, W., Chung, T. W., Kim, J. K., Park, J. G., Kang, H. K., Bom, H. S. & Yoon, J. H. (2007). "FDG PET/CT for the detection and evaluation of breast diseases: usefulness and limitations." *Radiographics* 27 Suppl 1: S197-213
- Lindholm, P., Lapela, M., Nagren, K., Lehtikainen, P., Minn, H. & Jyrkkio, S. (2009). "Preliminary study of carbon-11 methionine PET in the evaluation of early response to therapy in advanced breast cancer." *Nucl Med Commun* 30(1): 30-36
- Machulla, H. J., Blocher, A., Kuntzsch, M., Piert, M., Wei, R. & Grierson, J. R. (2000). "Simplified labeling approach for synthesizing 3'-deoxy-3'-[<sup>18</sup>F]fluorothymidine ([<sup>18</sup>F]FLT)." *Journal of Radioanalytical and Nuclear Chemistry* 243(3): 843-846
- Mahner, S., Schirmacher, S., Brenner, W., Jenicke, L., Habermann, C. R., Avril, N. & Dose-Schwarz, J. (2008). "Comparison between positron emission tomography using 2-[fluorine-18]fluoro-2-deoxy-D-glucose, conventional imaging and computed tomography for staging of breast cancer." *Ann Oncol* 19(7): 1249-1254
- Mariani, G., Bruselli, L. & Duatti, A. (2008). "Is PET always an advantage versus planar and SPECT imaging?" *Eur J Nucl Med Mol Imaging* 35(8): 1560-1565
- Moasser, M. M. (2007). "The oncogene HER2: its signaling and transforming functions and its role in human cancer pathogenesis." *Oncogene* 26(45): 6469-6487
- Mortimer, J. E., Dehdashti, F., Siegel, B. A., Trinkaus, K., Katzenellenbogen, J. A. & Welch, M. J. (2001). "Metabolic flare: indicator of hormone responsiveness in advanced breast cancer." *J Clin Oncol* 19(11): 2797-2803
- Munch-Petersen, B., Cloos, L., Jensen, H. K. & Tyrsted, G. (1995). "Human thymidine kinase 1. Regulation in normal and malignant cells." *Adv Enzyme Regul* 35: 69-89
- Orlova, A., Wallberg, H., Stone-Elander, S. & Tolmachev, V. (2009). "On the selection of a tracer for PET imaging of HER2-expressing tumors: direct comparison of a <sup>124</sup>I-labeled affibody molecule and trastuzumab in a murine xenograft model." *J Nucl Med* 50(3): 417-425
- Oude Munnink, T. H., Nagengast, W. B., Brouwers, A. H., Schroder, C. P., Hospers, G. A., Lub-de Hooge, M. N., van der Wall, E., van Diest, P. J. & de Vries, E. G. (2009). "Molecular imaging of breast cancer." *Breast* 18 Suppl 3: S66-73
- Peterson, L. M., Mankoff, D. A., Lawton, T., Yagle, K., Schubert, E. K., Stekhova, S., Gown, A., Link, J. M., Tewson, T. & Krohn, K. A. (2008). "Quantitative imaging of estrogen receptor expression in breast cancer with PET and <sup>18</sup>F-fluoroestradiol." *J Nucl Med* 49(3): 367-374

- Pio, B. S., Park, C. K., Pietras, R., Hsueh, W. A., Satyamurthy, N., Pegram, M. D., Czernin, J., Phelps, M. E. & Silverman, D. H. (2006). "Usefulness of 3'-[F-18]fluoro-3'-deoxythymidine with positron emission tomography in predicting breast cancer response to therapy." *Mol Imaging Biol* 8(1): 36-42
- Reske, S. N. & Deisenhofer, S. (2006). "Is 3'-deoxy-3'-(18)F-fluorothymidine a better marker for tumour response than (18)F-fluorodeoxyglucose?" *Eur J Nucl Med Mol Imaging* 33 Suppl 1: 38-43
- Romer, J., Fuchtnner, F., Steinbach, J. & Kasch, H. (2001). "Automated synthesis of 16alpha-[18F]fluoroestradiol-3,17beta-disulphamate." *Appl Radiat Isot* 55(5): 631-639
- Ruoslahti, E. & Pierschbacher, M. D. (1987). "New perspectives in cell adhesion: RGD and integrins." *Science* 238(4826): 491-497
- Sampath, L., Kwon, S., Ke, S., Wang, W., Schiff, R., Mawad, M. E. & Sevick-Muraca, E. M. (2007). "Dual-labeled trastuzumab-based imaging agent for the detection of human epidermal growth factor receptor 2 overexpression in breast cancer." *J Nucl Med* 48(9): 1501-1510
- Schechter, N. R., Yang, D. J., Azhdarinia, A. & Chanda, M. (2007). "Technologies for translational imaging using generators in oncology." *Recent Pat Anticancer Drug Discov* 2(3): 251-258
- Schilling, K., Narayanan, D., Kalinyak, J. E., The, J., Velasquez, M. V., Kahn, S., Saady, M., Mahal, R. & Chrystal, L. (2011). "Positron emission mammography in breast cancer presurgical planning: comparisons with magnetic resonance imaging." *Eur J Nucl Med Mol Imaging* 38(1): 23-36
- Schirrmeister, H. (2007). "Detection of bone metastases in breast cancer by positron emission tomography." *Radiol Clin North Am* 45(4): 669-676, vi
- Schirrmeister, H., Rentschler, M., Kotzerke, J., Diederichs, C. G. & Reske, S. N. (1998). "Skeletal imaging with (FNa)-F-18-PET and comparison with planar skeletal scintigraphy." *Rofo-Fortschritte Auf Dem Gebiet Der Rontgenstrahlen Und Der Bildgebenden Verfahren* 168(5): 451-456
- Scopinaro, F., Schillaci, O., Scarpini, M., Mingazzini, P. L., Di Macio, L., Banci, M., Danieli, R., Zerilli, M., Limiti, M. R. & Centi Colella, A. (1994). "Technetium-99m sestamibi: an indicator of breast cancer invasiveness." *Eur J Nucl Med* 21(9): 984-987
- Seitz, U., Wagner, M., Neumaier, B., Wawra, E., Glatting, G., Leder, G., Schmid, R. M. & Reske, S. N. (2002). "Evaluation of pyrimidine metabolising enzymes and in vitro uptake of 3'-[(18)F]fluoro-3'-deoxythymidine ([18F]FLT) in pancreatic cancer cell lines." *Eur J Nucl Med Mol Imaging* 29(9): 1174-1181
- Sharma, R., Tripathi, M., Panwar, P., Chuttani, K., Jaimini, A., Maitra, S., Chopra, M. K., Sawroop, K., Shukla, G., Mondal, A. & Mishra, A. (2009). "99mTc-methionine scintimammography in the evaluation of breast cancer." *Nucl Med Commun* 30(5): 338-342
- Shields, A. F., Grierson, J. R., Dohmen, B. M., Machulla, H. J., Stayanoff, J. C., Lawhorn-Crews, J. M., Obradovich, J. E., Muzik, O. & Mangner, T. J. (1998). "Imaging proliferation in vivo with [F-18]FLT and positron emission tomography." *Nat Med* 4(11): 1334-1336
- Spence, A. M., Muzi, M., Link, J. M., O'Sullivan, F., Eary, J. F., Hoffman, J. M., Shankar, L. K. & Krohn, K. A. (2009). "NCI-sponsored trial for the evaluation of safety and preliminary efficacy of 3'-deoxy-3'-[18F]fluorothymidine (FLT) as a marker of

- proliferation in patients with recurrent gliomas: preliminary efficacy studies." *Mol Imaging Biol* 11(5): 343-355
- Sundararajan, L., Linden, H. M., Link, J. M., Krohn, K. A. & Mankoff, D. A. (2007). "18F-Fluoroestradiol." *Semin Nucl Med* 37(6): 470-476
- Takada, Y., Ye, X. & Simon, S. (2007). "The integrins." *Genome Biol* 8(5): 215
- Tseng, J., Dunnwald, L. K., Schubert, E. K., Link, J. M., Minoshima, S., Muzi, M. & Mankoff, D. A. (2004). "18F-FDG kinetics in locally advanced breast cancer: correlation with tumor blood flow and changes in response to neoadjuvant chemotherapy." *J Nucl Med* 45(11): 1829-1837
- Wijns, W. & Camici, P. G. (1997). "The value of quantitative myocardial perfusion imaging with positron emission tomography in coronary artery disease." *Herz* 22(2): 87-95
- Winberg, K. J., Persson, M., Malmstrom, P. U., Sjoberg, S. & Tolmachev, V. (2004). "Radiobromination of anti-HER2/neu/ErbB-2 monoclonal antibody using the p-isothiocyanatobenzene derivative of the [76Br]undecahydro-bromo-7,8-dicarbanido-undecaborate(1-) ion." *Nucl Med Biol* 31(4): 425-433
- Xu, H., Baidoo, K., Gunn, A. J., Boswell, C. A., Milenic, D. E., Choyke, P. L. & Brechbiel, M. W. (2007). "Design, synthesis, and characterization of a dual modality positron emission tomography and fluorescence imaging agent for monoclonal antibody tumor-targeted imaging." *J Med Chem* 50(19): 4759-4765
- Yeh, K. A., Fortunato, L., Ridge, J. A., Hoffman, J. P., Eisenberg, B. L. & Sigurdson, E. R. (1995). "Routine bone scanning in patients with T1 and T2 breast cancer: a waste of money." *Ann Surg Oncol* 2(4): 319-324
- Yoo, J., Dence, C. S., Sharp, T. L., Katzenellenbogen, J. A. & Welch, M. J. (2005). "Synthesis of an estrogen receptor beta-selective radioligand: 5-[18F]fluoro-(2R,3S)-2,3-bis(4-hydroxyphenyl)pentanenitrile and comparison of in vivo distribution with 16alpha-[18F]fluoro-17beta-estradiol." *J Med Chem* 48(20): 6366-6378
- Yun, M., Oh, S. J., Ha, H. J., Ryu, J. S. & Moon, D. H. (2003). "High radiochemical yield synthesis of 3'-deoxy-3'-[18F]fluorothymidine using (5'-O-dimethoxytrityl-2'-deoxy-3'-O-nosyl-beta-D-threo pentofuranosyl)thymine and its 3-N-BOC-protected analogue as a labeling precursor." *Nucl Med Biol* 30(2): 151-157

IntechOpen



## **Breast Cancer - Recent Advances in Biology, Imaging and Therapeutics**

Edited by Dr. Susan Done

ISBN 978-953-307-730-7

Hard cover, 428 pages

**Publisher** InTech

**Published online** 14, December, 2011

**Published in print edition** December, 2011

In recent years it has become clear that breast cancer is not a single disease but rather that the term encompasses a number of molecularly distinct tumors arising from the epithelial cells of the breast. There is an urgent need to better understand these distinct subtypes and develop tailored diagnostic approaches and treatments appropriate to each. This book considers breast cancer from many novel and exciting perspectives. New insights into the basic biology of breast cancer are discussed together with high throughput approaches to molecular profiling. Innovative strategies for diagnosis and imaging are presented as well as emerging perspectives on breast cancer treatment. Each of the topics in this volume is addressed by respected experts in their fields and it is hoped that readers will be stimulated and challenged by the contents.

### **How to reference**

In order to correctly reference this scholarly work, feel free to copy and paste the following:

Fan-Lin Kong and David J. Yang (2011). Radiotracers for Molecular Imaging of Breast Cancer, Breast Cancer - Recent Advances in Biology, Imaging and Therapeutics, Dr. Susan Done (Ed.), ISBN: 978-953-307-730-7, InTech, Available from: <http://www.intechopen.com/books/breast-cancer-recent-advances-in-biology-imaging-and-therapeutics/radiotracers-for-molecular-imaging-of-breast-cancer>

**INTECH**  
open science | open minds

### **InTech Europe**

University Campus STeP Ri  
Slavka Krautzeka 83/A  
51000 Rijeka, Croatia  
Phone: +385 (51) 770 447  
Fax: +385 (51) 686 166  
[www.intechopen.com](http://www.intechopen.com)

### **InTech China**

Unit 405, Office Block, Hotel Equatorial Shanghai  
No.65, Yan An Road (West), Shanghai, 200040, China  
中国上海市延安西路65号上海国际贵都大饭店办公楼405单元  
Phone: +86-21-62489820  
Fax: +86-21-62489821

© 2011 The Author(s). Licensee IntechOpen. This is an open access article distributed under the terms of the [Creative Commons Attribution 3.0 License](https://creativecommons.org/licenses/by/3.0/), which permits unrestricted use, distribution, and reproduction in any medium, provided the original work is properly cited.

IntechOpen

IntechOpen